16th Australasian Fluid Mechanics Conference
Crown Plaza, Gold Coast, Australia
2-7 December 2007

Eigen-analysis of a Fully Viscous Boundary-Layer flow Interacting with a Finite Compliant Surface

M. W. Pitman and A. D. Lucey

Fluid Dynamics Research Group
Curtin University of Technology, Western Australia, 6845 AUSTRALIA

Abstract

A method and preliminary results are presented for the determination of eigenvalues and eigenmodes from fully viscous boundary layer flow interacting with a finite length one-sided compliant wall. This is an extension to the analysis of inviscid flow-structure systems which has been established in previous work. A combination of spectral and finite-difference methods are applied to a linear perturbation form of the full Navier-Stokes equations and one-dimensional beam equation. This yields a system of coupled linear equations that accurately define the spatio-temporal development of linear perturbations to a boundary layer flow over a finite-length compliant surface. Standard Krylov subspace projection methods are used to extract the eigenvalues from this complex system of equations. To date, the analysis of the development of Tollmien-Schlichting (TS) instabilities over a finite compliant surface have relied upon DNS-type results across a narrow (or even singular) spectrum of TS waves. The results from this method have the potential to describe conclusively the role that a finite length compliant surface has in the development of two-dimensional TS instabilities and other FSI instabilities across a broad spectrum.

Introduction

A numerical method is presented for the linear analysis of an incompressible, perturbed rotational flow at moderate Reynolds number interacting with a compliant surface. The linearised Navier-Stokes equations are used to represent the flow using a velocity-vorticity formulation that can accurately model perturbations without the need for turbulence models.

A schematic of the flow-structure system is presented in Figure 1. The rotational flow field that is studied in this case comprises a fully developed Poiseuille boundary layer flow between two plates. A finite compliant section of the lower plate, of length L, interacts with the rotational flow field. The finite length compliant section is composed of a simple elastic plate which may have a uniformly distributed spring foundations and structural damping added. The system is similar to the configuration used by Carpenter & Davies [2]. Although this work uses a Poiseuille mean flow profile, the robust computational method allows for the consideration of any mean flow profile and fluid-structure configuration.

Early work on compliant surfaces involved mainly analytical studies involving *infinite* compliant walls and inviscid, irrotational flow governed by Laplace's equation. In these cases, analytical solutions were obtained for the stability of the linearised flow structure system, e.g. see the work of Carpenter & Garrad [1].

Subsequent investigation of finite compliant walls comprised numerical studies such as Lucey & Carpenter [5]. These studies adapted panel methods for the solution of Laplace's equation in the fluid domain, with the structural solution obtained using finite-difference methods. Coupling of fluid pressures and structural forces permitted solution of the strongly coupled

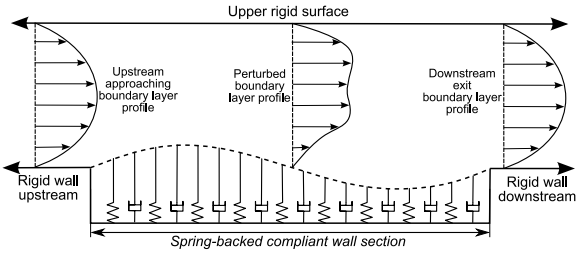

Figure 1: Schematic of the flow-structure system studied; the spring and dashpot foundations are absent for an unsupported elastic plate.

flow-structure system through a time-stepping routine.

Carpenter & Davies [2] introduced a rotational flow field, solving the linearly perturbed flow field in velocity-vorticity form and then numerically coupling this to the structural solution. The solution of the coupled equations adopted a time-stepping method similar to Lucey *et. al* [6] and therefore still produced results involving transient behaviour for a narrow set of initial or inlet conditions.

The use of Krylov subspace projection methods permit the extraction of eigenvalues and eigenvectors (modes) from large matrices. Ehrenstein & Gallaire [4] analysed the linear spatio-temporal disturbance evolution in a boundary layer with rigid walls. This study also formulated the fluid equations (Navier-Stokes) in velocity-vorticity form. Using the same techniques for extraction of eigenvalues, Lucey & Pitman [7] performed a similar linear analysis on an inviscid, finite-length, flow-structure compliant wall problem like that of Lucey *et al.* [6].

The first coupling of a discrete-vortex method for a gridless velocity-vorticity solution method, to a non-linearly deforming compliant wall was performed by Pitman [8]. This method accounted for non-linear effects and gave DNS-type results for the coupled system through a time-stepping solution.

The present work employs a linearised variation of the velocity-vorticity flow solution and coupling of Pitman [8] along with structural solution and eigenvalue extraction methods similar to Ehrenstein & Gallaire [4]. The strongly coupled model can be used to analyse the spatio-temporal disturbance evolution and global stability of fluid-structure systems, giving a broader spectrum of stability information than capable through the time-stepping solutions such as Carpenter & Davies [2].

Computational Method

A description of the computational method is presented below. First, the equations and solution method for the fluid domain are considered. The structural solution and coupling of the system through the forcing pressure is then presented.

Fluid domain

The flow field is modelled by the Navier-Stokes equations in linearised perturbation form as the continuity equation $\nabla.\vec{u}_p = 0$ and the linearised perturbation momentum equation

$$\left(\frac{\partial}{\partial t} + U\frac{\partial}{\partial x}\right)\vec{u}_p + v_p\frac{dU}{dy} = -\nabla p + \nu\left(\nabla^2\vec{u}_p\right) \ , \qquad (1)$$

where u_p and v_p are the velocity perturbation fields in the x and y direction respectively. Equation 1 may be expressed in velocity-vorticity form, with a mean-flow velocity profile in the x and y directions denoted U_m and V_m respectively, the mean-flow vorticity field given by $\Omega_\infty(x,y)$, and the perturbation vorticity field denoted ω_p. Maintaining an Eulerian reference frame this becomes

$$\frac{\partial\omega}{\partial t} + U_m\frac{\partial\omega_p}{\partial x} + u_p\frac{\partial\Omega_\infty}{\partial x} + V_m\frac{\partial\omega_p}{\partial y} + v_p\frac{\partial\Omega_\infty}{\partial y} = \nu\nabla^2\omega_p \ . \qquad (2)$$

This formulation is seen in the work of Davies & Carpenter [3]. For a plane parallel mean flow profile where $V_m = 0$ and $U_m = f(y)$ then Equation 2 becomes

$$\frac{\partial\omega}{\partial t} + U_m\frac{\partial\omega_p}{\partial x} + v_p\frac{\partial\Omega_\infty}{\partial y} = \nu\nabla^2\omega_p \ . \qquad (3)$$

The no-slip boundary condition is enforced through the injection of slip-velocity at the wall. Flow field elements close to the wall therefore have an added term to the right hand side of Equation 3 which adds vorticity to these elements based upon the vector, $\{u_s\}$, of slip velocities at the wall. This takes the form of $[C_{SV}]\{\dot{u}_s\}$, where $[C_{SV}]$ is a matrix that converts the measured slip velocity to the required amount of vorticity to add.

The flow field is spatially discretised into rectangular elements. The vorticity contained within each rectangular element is approximated by a zero-order vortex sheet element. A vector of flow field element strengths is defined as $\{\omega_f\}$. These singularity element strengths are related to the distributed vorticity field as $\{\omega_f\} = [K]\{\omega\}$, where $[K]$ is a matrix relating the distributed vorticity field at control points, $\{\omega\}$, to the singularity strengths. Likewise, singularity elements which enforce the no-flux condition at the flow structure interface are approximated by source(-sink) sheet elements, and a vector of wall element singularity strengths is defined as $\{\sigma\}$. The vector of y-direction perturbation velocities, v_p in Equation 3, is then

$$\{v_p\} = [I_{Vff}]\{\omega_f\} + [I_{Vwf}]\{\sigma\} \ , \qquad (4)$$

where $[I_{Vff}]$ and $[I_{Vwf}]$ are influence-coefficient matrices for the y-direction velocity due to flow elements onto themselves and wall elements onto flow elements respectively.

The strength of the wall singularity strengths is determined through enforcing the no-flux boundary condition at the wall.

$$\{\sigma\} = [I_N]^{-1}\{\dot{\eta}\} - [I_N]^{-1}[I_{Nfw}]\{\omega_f\} \ , \qquad (5)$$

where $[I_N]$ is a matrix of the normal influence coefficients at the wall from the wall singularity elements, $\{\dot{\eta}\}$ is a vector of wall node displacements and $[I_{Nfw}]$ is a matrix of normal velocity influence coefficients of the flow elements onto the wall.

Substituting Equation 5 into Equation 4 gives the complete expression for y-direction perturbation velocity as

$$\{v_p\} = [A]\{\dot{\eta}\} + [B]\{\omega_f\} \ , \qquad (6)$$

where

$$[A] = [I_{Vwf}][I_N]^{-1}$$
$$[B] = \left[[I_{Vff}] - [I_{Vwf}][I_N]^{-1}[I_{Nfw}]\right] \ .$$

The amount of vorticity injection at the wall is based on the amount of slip velocity that is accumulated at the wall. The amount of slip velocity at the wall is expressed as

$$\{u_s\} = [I_{Tfw}]\{\omega_f\} + [I_T]\{\sigma\} \ , \qquad (7)$$

where $[I_{Tfw}]$ is a matrix of influence coefficients relating flow field singularity elements to tangential velocity at the wall and $[I_T]$ is a tangential velocity influence coefficient matrix for singularity strengths at the wall. The vector of wall singularity strengths is defined by Equation 5. Substituting Equation 5 into Equation 7 gives an expression for slip velocity at the wall as

$$\{u_s\} = [C]\{\dot{\eta}\} + [D]\{\omega_f\} \ . \qquad (8)$$

where

$$[C] = [I_T][I_N]^{-1}$$
$$[D] = \left[[I_{Tfw}] - [I_{Vwf}][I_N]^{-1}[I_{Nfw}]\right] \ .$$

The influence coefficients are constant, therefore the rate of change of u_s at the wall is given by

$$\{\dot{u}_s\} = [C]\{\ddot{\eta}\} + [D]\{\dot{\omega}_f\} \ . \qquad (9)$$

Equation 6 may be substituted into Equation 3 to obtain a complete linearised expression for the discretised system with moving boundaries in matrix form, with Equation 9 enforcing the no-slip boundary condition at the wall.

Structural solution

The linear motion of the compliant wall is governed by the two-dimensional beam equation. Extra terms are added to account for the addition of homogeneous backing springs ($K\eta$) and uniform dashpot-type damping ($d\partial\eta/\partial t$) to model the effects of energy dissipation in the wall structure.

$$\rho_m h\frac{\partial^2\eta}{\partial t^2} + d\frac{\partial\eta}{\partial t} + B\frac{\partial^4\eta}{\partial x^4} + K\eta = -\Delta p(x,0,t) \ , \qquad (10)$$

where $\eta(x,t)$, ρ_m, h and B are, respectively, the plate's deflection, density, thickness and flexural rigidity, while $p(x,y,t)$ is the unsteady fluid pressure. In the present problem we apply hinged-edge conditions at the leading and trailing edges of the plate although in the method that follows there is no necessary restriction on such boundary conditions.

Pressure and Coupling

The pressure may be determined at the compliant wall section through a variety of means. In this study, the pressure is determined simultaneously with the slip velocity in Equation 7 through the Lighthill mechanism which relates streamwise pressure gradient with the injected flux of vorticity. The pressure at the wall is therefore related to the slip velocity through $\{p\} = [C_{PS}]\{\dot{u}_s\}$, where $\dot{u}_s$ is given by Equation 9 and $[C_{PS}]$ is an integration matrix along the lower wall. The interfacial pressure (on the right hand side of Equation 10) may therefore be expressed in the form

$$\{p\} = [E]\{\ddot{\eta}\} + [F]\{\dot{\omega}_f\} \ , \qquad (11)$$

where $[E]$ and $[F]$ are coefficient matrices formed from the product of $[C_{PS}]$ with $[C]$ and $[D]$ in Equation 9 respectively.

Equation 11 along with Equations 10, 9, 6 and 3 permit the entire flow-structure system to be expressed as a linear system for a single set of unknowns comprising the flow-field vorticity,

$\{\omega_f\}$ and the wall node displacements, $\{\eta\}$. The entire flow-structure system may therefore be reduced to a first order linear differential equation of the form

$$[C_1]\{\dot{\Gamma}\} = [C_2]\{\Gamma\} \quad , \tag{12}$$

where $\{\Gamma\}$ is a vector of system variables comprising the flow field elements, $\{\omega_f\}$, the wall node displacments, $\{\eta\}$ and the wall node velocities $\{\dot{\eta}\}$. $[C_1]$ is the matrix product of all coefficients relating the rate of change of element strengths obtained from Equations 3, 10 and 11. The matrix $[C_2]$ is similarly the matrix product of all coefficients relating the element strengths.

Matrices C_1 and C_2 are square dense matrices of dimension $M+2N$, where M is the number of elements that are used to discretise the flow field and N is the number of elements used to discretise the wall.

Solution Methodology

Equation 12 expresses the entire flow structure system as a set of coupled linear first order differential equations. Standard linear analysis techniques may be applied to this set of equations in order to extract system information such as stability bounds, eigenvalues and eigenmodes. Difficulties arise in the extraction of this information because: a) the number of coupled equations is large, with the number of discrete flow field elements $M \approx 12000$ for the fluid domain and $N = 400$ for the structural domain, and b) the equations are *not* sparse, although they are dense on the diagonal.

The above points make extraction of eigenvalues computationally expensive as compared to the effor required for sparse diagonal matrices that would result from a finite element or finite difference solution of the flow field in primitive (u,v,p) variables. However, development of the system equations using primitive variables such as this would require much finer grid resolution in order to capture high Reynolds-number flow instabilities, resulting in much larger matrices on which the analysis must be performed.

The equations are couched in finite difference form for the streamwise representation while Chebyshev differentiation matricies are used to express the differential equations in the wall-normal direction. The use of mixed finite-difference and Chebyshev-differentiation matricies is more effective due to the high elemental aspect ratio, which suffers from numerical instability if finite difference representation alone is used in both directions.

Various computational algorithms are available which permit the extraction of eigenvalues and eigenvectors from large systems of equations such as Equation 12. In this study, the ARPACK package of FORTRAN libraries is implemented through the MATLAB software. ARPACK is an algorithmic variant of the Arnoldi process, which is based on Krylov subspaces. This permits extraction of global system eigenvalues and eigenmodes from very large systems of linear equations. The method does not however return *all* of the system eigenvalues and eigenmodes, rather it returns a specific subset of all possible eigenvalues and their corresponding modes.

Determination of all system eigenvalues and eigenmodes would not be desirable in this case due to the large number of equations (yielding ≈ 15000 eigenvalues and eigenmodes), causing problems with storage and data processing. Typically we are interested in only a subset that meet a specific criteria such as the eigenvalues with the largest real part (most unstable).

Preliminary results

This paper focusses on developing the method for linear analysis of a boundary layer with a compliant wall and presents a few results that demonstrate its sucessful implementation. A comprehensive study of the flow-structure problem utilising this method is left for future work.

Herein we solve for the flow field only and therefore keep the walls rigid (or the flexural rigidity B very high). In these intial results only 16 node points were used in the Chebyshev collocation grid in the wall-normal direction, while 200 node points were used for the finite difference representation in the streamwise direction. Likewise 200 boundary elements were used to enforce the no-flux condition at the wall. Both the upper and lower walls are rigid. Figure 2 shows an example of the Chebyshev collocation grid in the wall normal direction, with the lower wall lying at $y = 0$ and the upper wall at $y = 0.03$. The grid is linearly transformed slightly to provide a higher resolution near the lower (compliant) wall.

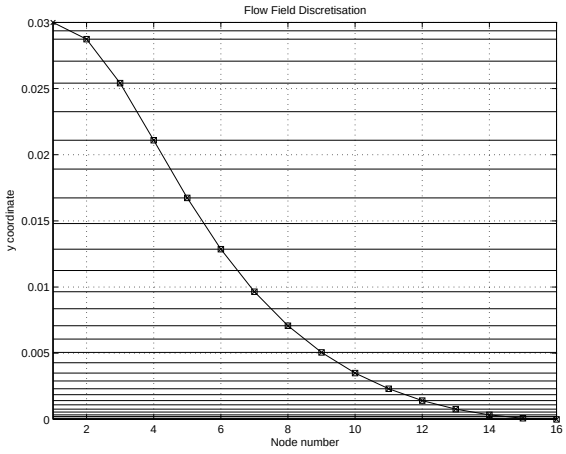

Figure 2: Discretisation of in the wall normal direction using a Chebyshev-collocation grid. x = element node points (edges of the rectangular elements), the horizontal lines highlight the element centres and node point positions respectively.

Figure 3 shows a colour plot for the values of the first 200×200 elements of the coefficient matrix that defines the perturbation velocity v_p, multiplied by the mean-vorticity gradient, $d\Omega/dy$, in Equation 3. This term contributes heavily to the vertical perturbation vorticity transport throughout the fluid domain. The other terms that contribute to the right hand side coefficient matrix (C_2) are the streamwise perturbation vorticity convection, $U\partial\omega_p/\partial x$, and the perturbation vorticity diffusion, $\nu[D_2]\omega$. The density of the matrix as a result of the velocity-vorticity formulation that is used may be seen in Figure 3.

Figure 4 a colour plot for the values of the first 200×200 elements of the coefficient matrix of the left hand side of Equation 12 ($[C_1]$). As with Figure 3, it can be seen that the matrix is dense and not sparse on the diagonal. This matrix C_1 has the added complexity of horizontal streaks throughout the matrix. This horizontal streaking is a result of the vorticity injection term that counters the production of slip velocity at the wall and thereby enforces the no-slip condition ($u_p = 0$ at $y = 0$).

Figure 5 shows contour plots for the vorticity distribution over half the channel flow at three times throughout an explicit time-stepping solution of the linear system defined by Equation 12. A small amount of vorticity is set at position $x = 0.125, y = 0.0225$ for the initial condition. These results indicate show that the initial package of vorticity convects downstream and diffuses

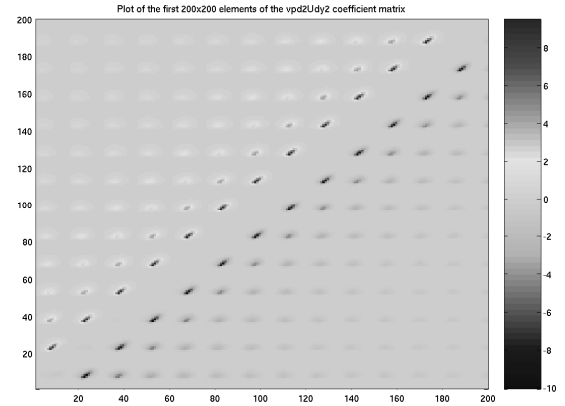

Figure 3: Values of the first 200×200 elements of the coefficient matrix for $v_p \partial^2 U / \partial y^2$

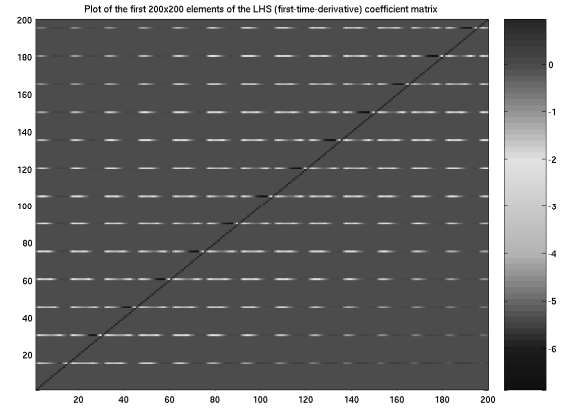

Figure 4: Values of the first 200×200 elements of the coefficient matrix for the left hand side of Equation 12, $[C_1]$

in both the x and y directions qualitatively correctly. It also indicates that the wall interface is reacting to enforce the no-flux and no-slip condition through injection of vorticity at the wall. These results indicate that the linear modelling technique described in this paper is able to generate qualitatively correct results. Further validation is required before the solution of system eigenvalues and eigenmodes using the ARPACK routine is performed. These results indicate that the system is well-posed for this solution method and therefore linear analysis of the spatio-temporal system should be straight forward to implement.

Conclusions

This paper has presented a new solution method for the linear analysis of moderate reynolds number flows interacting with a compliant surface. The preliminary results show that the computational method is robust and leaves a system of equations that are well-posed for linear analysis and eigenvalue extraction through Krylov subspace projection methods.

Acknowledgements

We would like to acknowledge the cooperation of the Fluid Dynamics Research Centre (FDRC) at Warwick University, UK. This research is supported by the Australian Research Council (ARC) through the Discovery Projects scheme.

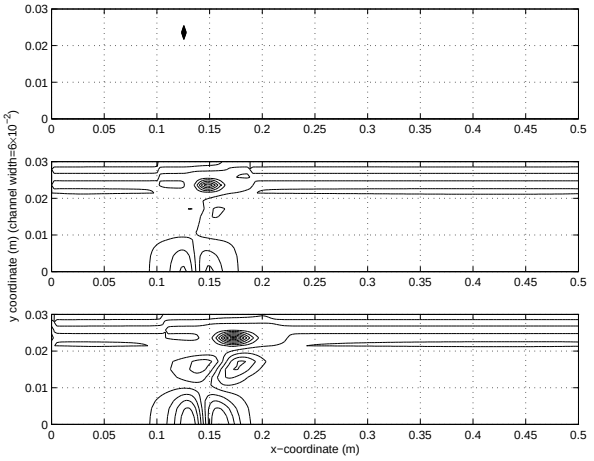

Figure 5: Contours of vorticity in the flow field for the development of a packet of vorticity throughout time. Snapshots of vorticity distribution are at times $t = 0, t = 25 \times 10^{-3}$ and $t = 50 \times 10^{-3}$ respectively.

References

[1] Carpenter, P.W. and Garrad, A.D., The hydrodynamic stability of flows over Kramer-type compliant coatings. Part 1. Tollmien-Schlichting instabilities. *Journal of Fluid Mechanics*, **155**, 1985, 465–510.

[2] Carpenter, P.W. and Davies, C., Numerical simulation of the evolution of Tollmien-Schlichting waves over finite compliant surfaces. *Journal of Fluid Mechanics*, **335**, 1997, 361–392.

[3] Davies, C. and Carpenter, P.W., A Novel Velocity-Vorticity Formulation of the Navier-Stokes Equations with Applications to Boundary Layer Disturbance Evolution. *Journal of Computational Physics*, **172**, 2001, 119–165.

[4] Ehrenstein, U. and Gallaire, F., On two dimensional temporal modes in spatially evolving open flows: the flat plate boundary layer. *Journal of Fluid Mechanics*, **536**, 2005, 209–218.

[5] Lucey, A. D. and Carpenter, P.W., A numerical simulation of the interaction of a compliant wall and an inviscid flow. *Journal of Fluids Mechanics*, **234**, 1992, 121–146.

[6] Lucey, A. D., Carpenter, P.W., Cafolla, G. J. and Yang, M., The Nonlinear Hydroelastic Behaviour of Flexible Walls. *Journal of Fluids and Structures*, **11**, 1997, 717–744.

[7] Lucey, A.D. and Pitman, M.W., A new method for determiningn the eigenmodes of finite flow-structure systems. Paper no. pvp2006-icpv11-93938. In proceedings of: *ASME-PVP 2006: 2006 ASME Pressure Vessels and Piping Division Conference*, July 23-27, 2006, CD-ROM (4 pages).

[8] Pitman, M.W., An investigation of flow structure interactions on a finite compliant surface using computational methods. *Ph.D. Thesis, Curtin University of Technology*, 2007.